Catal Lett (2009) 128:1–8
DOI 10.1007/s10562-008-9754-4

Dependence of Gas-Phase Crotonaldehyde Hydrogenation Selectivity and Activity on the Size of Pt Nanoparticles (1.7–7.1 nm) Supported on SBA-15

Michael E. Grass · Robert M. Rioux · Gabor A. Somorjai

Received: 1 October 2008 / Accepted: 23 October 2008 / Published online: 26 November 2008

Abstract The selectivity and activity for the hydrogenation of crotonaldehyde to crotyl alcohol and butyraldehyde was studied over a series of Pt nanoparticles (diameter of 1.7, 2.9, 3.6, and 7.1 nm). The nanoparticles were synthesized by alcohol reduction of a Pt salt in the presence of poly(vinylpyrrolidone) (PVP), followed by incorporation into mesoporous SBA-15 silica. The rate of crotonaldehyde hydrogenation and selectivity towards crotyl alcohol both increase with increasing particle size. With an increase in particle size from 1.7 nm to 7.1 nm, the selectivity towards crotyl alcohol increases from 13.7% to 33.9% (8 Torr crotonaldehyde, 160 Torr H_2 and 353 K). The turnover frequency increases from 2.1×10^{-2} s^{-1} to 4.8×10^{-2} s^{-1} with increasing particle size. Additionally, the decarbonylation pathway to form propene and CO is enhanced over smaller nanoparticles. The apparent activation energy remains constant ($\sim$16 kcal mol^{-1} for the formation of butyraldehyde and $\sim$8 kcal mol^{-1} for the formation of crotyl alcohol) as a function of particle size as does the reaction order in H_2, which is unity. In the presence of 130–260 mTorr CO, the reaction rate decreases for all products with a CO reaction order of -1 to -1.4 for crotyl alcohol and butyraldehyde. Hydrogen reduction at 673–723 K results in increased activity and selectivity relative to reduction at either higher or lower temperature; this is discussed with respect to the organic capping agent, PVP.

Keywords Crotonaldehyde · Hydrogenation · Platinum · Nanoparticles · Selectivity · Decarbonylation

M. E. Grass · R. M. Rioux · G. A. Somorjai (✉)
Lawrence Berkeley National Laboratory and Department of Chemistry, University of California, Berkeley, California 94720, USA
e-mail: somorjai@berkeley.edu

Present Address:
M. E. Grass
Advanced Light Source, Lawrence Berkeley National Laboratory, Berkeley, CA 94720, USA

Present Address:
R. M. Rioux
Department of Chemical Engineering, Pennsylvania State University, University Park, PA 16802-4400, USA

1 Introduction

Polymer and surfactant stabilized transition metal nanoparticles (NPs) have been utilized as both homogeneous and heterogeneous catalysts over the past decade [1]. Their catalytic ability has been studied extensively both as colloidal suspensions [2] and as oxide- or carbon-supported NPs [3, 4]. The polymer mediated method of catalyst preparation can yield transition metal NPs with narrow particle size distribution and thus has the potential to serve as model systems for the elucidation of particle size effects in catalysis.

In our previous work, we developed two strategies for supporting PVP-protected Pt nanoparticles on mesoporous SBA-15 silica and studied the particle size dependence of the single product reactions (ethylene hydrogenation and ethane hydrogenolysis) and the influence of particle size on the poisoning of ethylene hydrogenation by carbon monoxide.[5–9] In this paper, we report on the selective hydrogenation of crotonaldehyde to crotyl alcohol and butyraldehyde over a series of Pt(X)/SBA-15 (X = 1.7, 2.9, 3.6, and 7.1 nm) catalysts prepared by nanoparticle encapsulation (NE) [6]. We examined the effect of particle size for both the overall conversion of crotonaldehyde and

the selectivity towards the industrially desired unsaturated alcohol, crotyl alcohol. We demonstrate NE synthesized catalysts have similar catalytic activity and selectivity for crotonaldehyde hydrogenation as conventionally-prepared (insipient wetness, ion-exchange, etc.) catalysts [10].

The hydrogenation of crotonaldehyde and other α,β-unsaturated aldehydes is of fundamental scientific interest because two different types of unsaturated chemical bonds (C=C and C=O) are present in the same molecule, serving as a useful probe of heterogeneous catalytic chemoselectivity (Scheme 1). Gallezot and Richard summarized many of the properties that determine catalytic activity and selectivity for the conversion of α,β-unsaturated aldehydes by heterogeneous catalysts [10]. Properties of the catalyst that influence both activity and selectivity include the type of metal, the exposed crystal faces of the extended single-crystal or nanoparticle surface, adsorbed ligands (e.g. organometallic tin) and promoters (e.g. K, Fe, Sn) which modify the metal surface electronically and/or geometrically. The structure of the α,β-unsaturated aldehyde can also influence the reaction selectivity: bulky side groups such as the phenyl group adjacent to the double bond in cinnamaldehyde or the pair of methyl groups in 3-methyl-crotonaldehyde lead to higher selectivity for the corresponding unsaturated alcohol because of steric hindrance. In the case of crotonaldehyde, the C=C double bond is flanked by a methyl group only, and the selective hydrogenation of the carbonyl group over the C=C double bond becomes significantly more challenging [10].

In previous investigations of the influence of particle size on the overall turnover frequency (TOF) and selectivity for crotyl alcohol from crotonaldehyde, both generally increase with increasing particle size [11–13]. The role of particle size appears to be three-fold. The first is related to the fraction of exposed atoms in close packed (111) planes versus those at coordinatively unsaturated sites or in open faces such as (100) or (110). Crotonaldehyde preferentially adsorbs via a di-σ bond of C=O on the (111) surface of Pt, while on the (100) surface, it bonds to the surface in a flat geometry (η^4 configuration) through both of its π-bonds [14]. On the (110) surface, the most corrugated of the three lowest energy fcc surfaces, crotonaldehyde bonds via its C=C π-bond [14]. The increase in selective C=O interaction on (111) facets is responsible for the increased selectivity towards the unsaturated alcohol. Larger nanoparticles have a larger fraction of atoms in terraces with a close packed structure than smaller particles and are selective for the formation of crotyl alcohol [13]. The second reason for particle size dependent selectivity is the steric hindrance of the C=C bond, which is more easily accommodated on smaller NPs. Catalytic activity is also lower over smaller NPs because decarbonylation of crotonaldehyde to CO and C_3 hydrocarbons as well as other C–C bond breaking reactions occur preferentially on the corner and edge sites that are more prevalent on smaller particles: CO and carbon deposits from C–C bond breaking poison the catalyst surface.

For the investigation of gas-phase heterogeneous catalysis using stabilized NPs on oxide supports, organic capping molecules have typically been removed by thermal treatment [5, 15, 16]. In this investigation, we consider the effects of such thermal treatments on the final state of the capping polymer PVP and its implication for catalysis.

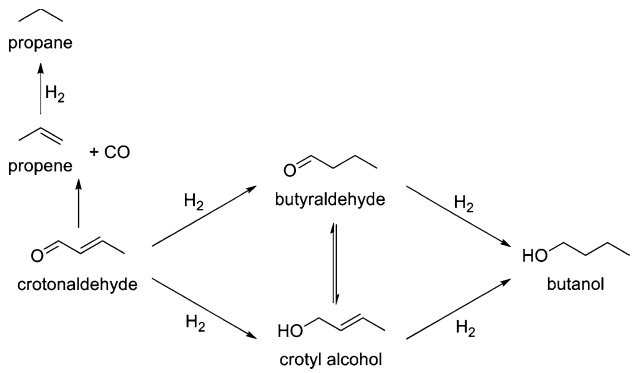

Scheme 1

2 Experimental

2.1 Catalyst Synthesis

The preparation of the Pt nanoparticles (NPs) used in this study and their anchoring in mesoporous SBA-15 silica by nanoparticle encapsulation (NE) has been reported previously [5, 6]. In this study, a series of Pt(X)/SBA-15 (X = 1.7–7.1 nm) were synthesized with nominal loadings of 1–3%. Higher weight loading of Pt was used for the catalysts containing larger NPs to account for the decrease in the total surface area of larger NPs compared to catalysts containing smaller nanoparticles at comparable weight loading. The 1.7 and 7.1 nm NPs were synthesized by the polyol reduction process in ethylene glycol (EG) [5, 17, 18], while 2.9 and 3.6 nm particles were synthesized in an 80/20 v/v mixture of methanol and water by alcohol reduction [5, 19]. The 3.6 nm particles were synthesized by a seeded growth method beginning with the 2.9 nm particles [19]. All of the NPs except for the 1.7 nm particles were synthesized in the presence of PVP, which sterically protects the particles from agglomeration [20]. The 1.7 nm particles are electrostatically stabilized in a solution of NaOH in EG during synthesis, then precipitated from the EG solution and transferred to an ethanol solution containing PVP.

The nanoparticles were incorporated into silica by synthesizing the mesoporous SBA-15-like silica matrix in neutral pH hydrothermal conditions in the presence of the PVP-protected NPs [6]. The catalysts were washed in ethanol, dried in air at 373 K and calcined ex situ in O_2 at 723 K for 12 h (Pt(2.9 nm)/SBA-15 and Pt(3.6 nm)/SBA-15), at 623 K for 12 h (Pt(1.7 nm)/SBA-15), or at 723 K for 24 h (Pt(7.1-15)/SBA-15) [5]. After calcination, the catalysts were characterized by X-ray diffraction (XRD) with a Bruker D8 GADDS diffractometer with Co K_α radiation ($\lambda = 1.79$ Å) and transmission electron microscopy (TEM, Philips/FEI Tecnai 12 microscope operated at 100 kV) for confirmation of the bulk particle size. The total surface area and metallic surface area were measured by N_2 physisorption (BET method) and H_2 chemisorption with a Quantachrome Autosorb 1 automated sorption analyzer. The catalysts were reduced in situ prior to chemisorption by the same protocol used for the reduction of catalysts in reaction studies (673 K in H_2 for 2 h) followed by evacuation at 623 K for 1 h. The catalyst was then cooled to 303 K under vacuum followed by volumetric chemisorption measurements. The total metal content was determined by inductively coupled plasma–optical emission spectroscopy (ICP-OES) at Galbraith Laboratories (Knoxville, TN USA).

2.2 Catalytic Studies

Catalytic reactions were carried out in a stainless steel (1/8″) flow reactor system equipped with mass flow controllers (MKS Instruments) for He, H_2, and O_2 (UHP, Praxair, used as-received) and an inline Pyrex saturator for the introduction of crotonaldehyde (Sigma-Aldrich, 99.9%, predominately *trans*) into the feed. The catalyst was reduced in situ at the desired temperature (typically 673 K) for 2 h in H_2 (160 Torr)/He (70 mL min^{-1}). The reaction was initiated by introducing a flow of 160 Torr H_2/He (70 mL min^{-1}) through the saturator containing crotonaldehyde held at 273 K. The inlet conditions prior to contact with the catalyst bed was 8 Torr crotonaldehyde, 160 Torr H_2 and balance He.

The catalyst was placed on top of a quartz frit in a 1/4″ O. D. Pyrex U-tube reactor. For a typical experiment, ~15 mg catalyst was diluted with ~50 mg acid-washed and calcined low surface area quartz (Sigma-Aldrich) and loaded into the reactor between beds of the same acid-washed and calcined quartz. The effluent stream was analyzed by gas chromatography (HP 5890 Series II) using a flame ionization detector (FID) for analysis of organics and a thermal conductivity detector (TCD) for H_2 detection. The reaction was started at 353 K until a stable activity was measured (i.e. until initial deactivation was complete and a steady-state activity was reached); most catalysts required ~2.5 h to reach steady-state. The reaction temperature was then changed (and left for 1.5 h at each temperature) to 373, 393, 383, 373, 363, and finally back to 353 K for a check on the extent of catalyst deactivation. Unless stated otherwise, data reported in this paper is the steady-state rate at 353 K (the deactivation check measurement). The activation energy for all samples was determined using the rates obtained while cooling from 393 to 353 K, averaging the rate calculated from ten GC injections at each temperature.

CO poisoning experiments were conducted at 353 K in the same manner described above, but with the addition of 1% CO in He (Praxair, UHP) controlled with a mass flow controller to correspond to CO pressures of 134–262 mTorr in the feed stream (total flow rate of 70 cc(NTP) min^{-1}).

The TOF was calculated by normalizing the reaction rate to the number surface Pt atoms based on TEM measurements and the Pt loading determined by ICP–OES. Selectivity values were calculated by dividing the TOF a particular product by the overall TOF (the rate of disappearance of crotonaldehyde).

3 Results and Discussion

3.1 Catalyst Properties

The as-synthesized NPs were analyzed by TEM and XRD before encapsulation and the SBA-15-supported Pt catalysts were characterized by ICP-OES, TEM, XRD, and chemisorption after calcination. An exhaustive analysis of the characteristics of these catalysts has been given previously and no notable deviations from the previous report were observed [6]. The metal loading determined by ICP–OES analysis, the metal dispersion determined from H_2 chemisorption measurements, and a summary of the catalytic results are listed in Table 1. The particle size determined from TEM and XRD line-broadening (determined using the Scherrer equation) are in agreement and analysis of the TEM images indicates a standard deviation in particle size of ~10% for all catalysts (Table 1).

The dispersions measured by irreversible hydrogen chemisorption are ~50% lower than the measured TEM results. The theoretical H/Pt_T (total Pt) ratio for 1.7, 2.9, 3.6, and 7.1 nm Pt NPs are 0.66, 0.39, 0.31, and 0.16, respectively, assuming hemispherical particles and 1:1 stoichiometry between H and Pt_s (surface Pt). This discrepancy suggests that the *ex situ* calcination-in situ reduction procedure described in the experimental section produce catalysts capable of adsorbing hydrogen up to only 50% coverage relative to the total number of surface Pt atoms, regardless of particle size (no sintering was observed by TEM). The suppressed adsorption of hydrogen

Table 1 Physiochemical properties and summary of catalytic results for Pt(X)/SBA-15 catalysts

Catalyst	Pt Loading[a] (% Pt)	TEM size (nm)	H/Pt[b]	TOF ($100 \times s^{-1}$)[c]	$S_{\text{crotyl alcohol}}$[d]	E_a (kcal mol^{-1})[e]
Pt(1.7)/SBA-15	0.58	1.7	0.33	2.1	13.7	10.8
Pt(2.9)/SBA-15	1.28	2.9	0.18	2.9	17.0	11.2
Pt(3.6)/SBA-15	1.61	3.6	0.15	4.3	21.6	10.8
Pt(7.1)/SBA-15	2.43	7.1	0.08	4.8	33.9	11.7

[a] Loading determined by ICP-OES

[b] Irreversible H_2 chemisorption at 303 K, extrapolated to $P = 0$

[c] Overall crotonaldehyde hydrogenation rate per surface site at 8 Torr C_6H_4O, 160 Torr H_2 and 353 K

[d] Determined at 8 Torr crotonaldehyde, and 160 Torr H_2 and 353 K

[e] Overall apparent activation energy determined at 8 Torr crotonaldehyde, 160 Torr H_2, and 353–393 K

is likely due to residual carbonaceous material from the decomposition of PVP during the oxygen and hydrogen pretreatment steps. It is interesting that the fractional coverage of this layer as measured by H_2 chemisorption is independent of particle size. In a study by Du, et al. [21] 2.5 nm PVP-protected Pt nanoparticles were heated in N_2 for 0.5 h and analyzed for elemental composition. After the heat treatment, the molar ratio of C to surface Pt is 35 (before thermal treatment, the ratio is 85). In this work, we have used oxygen pretreatment for a much longer time (12–24 h), but it appears that residual carbon from either PVP or P123 remains on the Pt surface. The surface coverage and chemical composition of this layer may play a significant role in the catalytic properties of these materials.

3.2 Crotonaldehyde Hydrogenation

Butyraldehyde is the major product of crotonaldehyde hydrogenation over all catalysts and the entire temperature range (353–393 K) studied, which forms by the selective hydrogenation of the C=C bond. The minor products are crotyl alcohol (the second most abundant product) formed by selective hydrogenation of the C=O bond, butanol (complete hydrogenation of C=C and C=O), and propylene and propane (decarbonylation) (Scheme 1).

The initial time-on-stream data for Pt(1.7 nm)/SBA-15 and Pt(7.1 nm)/SBA-15 shows an initial deactivation period that lasts about 2.5 h. It is well-documented in the literature that this deactivation is a result of decarbonylation and the subsequent adsorption of CO to the Pt surface, as well as carbon deposition resulting from C–C and C–H bond scission [22–25]. C_3 hydrocarbons produced from the decarbonylation pathway were detected at all reaction temperatures and on all catalysts, indicating the formation of CO. The initial TOF for decarbonylation is at least 10^{-3} s^{-1} for all four catalysts. If we assume that all of the CO formed by decarbonylation remains on the surface, enough CO forms to saturate the Pt surface sites (based on TEM dispersion measurements) within 15–20 min after the start of the reaction. The deactivation of heterogeneous catalysts for the hydrogenation of α,β-unsaturated aldehydes by CO as a result of decarbonylation has been revealed in surface science studies [25], infrared spectroscopy studies on supported catalysts [23], and through kinetic studies [24] over a number of different transition metals. A second pathway for deactivation is coke formation from C–C bond rupture. This process may be slower than CO formation through decarbonylation, but the products of this process will not desorb during reaction.

The temperature dependence for hydrogenation is similar for all catalysts studied. The overall apparent activation energy for the disappearance of crotonaldehyde is independent of the particle size (Table 1). The apparent activation energy for the individual products is also not dependent on particle size: 16–17 kcal mol^{-1} for C=C hydrogenation to butyraldehyde, 7–10 kcal mol^{-1} for C=O hydrogenation to crotyl alcohol, 10–15 kcal mol^{-1} for the complete hydrogenation to butanol, and 11–12 kcal mol^{-1} for decarbonylation. The temperature dependence for all products catalyzed by Pt(7.1 nm)/SBA-15 is presented in Fig. 1. Lower temperatures favor the formation of minor products, particularly crotyl alcohol, relative to butyraldehyde (the activation energy for the formation of butyraldehyde is lower than for the formation of crotyl alcohol over all catalysts studied). Butyraldehyde is the more thermodynamically-favored product, but it is also the more kinetically-hindered (higher apparent activation energy). The reaction order in H_2 (not shown) was unity at 353 K. These observations are consistent with general trends of crotonaldehyde hydrogenation over Pt catalysts that have been reported previously [10].

3.3 Particle Size Effects on Selectivity and Activity for Crotonaldehyde Hydrogenation

The steady-state TOF and reaction selectivity to crotyl alcohol at 353 K for all catalysts is listed in Table 1 and

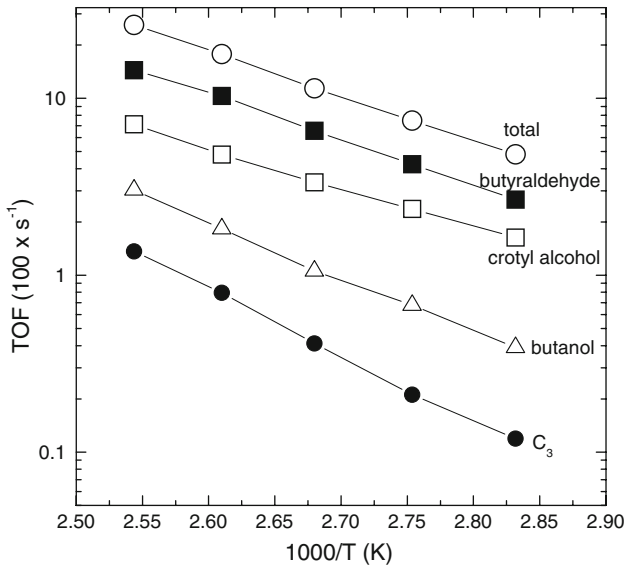

Fig. 1 Turnover frequency for the disappearance of crotonaldehyde (○) and formation of butyraldehyde (■), crotyl alcohol (□), butanol (Δ), and C_3 hydrocarbons (●) as an Arrhenius plot for Pt(7.1 nm)/SBA-15. The pressure of crotonaldehyde and hydrogen was 8 Torr and 160 Torr (760 Torr total pressure). The apparent activation energies are 12 kcal mol^{-1} overall, 17 kcal mol^{-1} for the formation of butyraldehyde, 10 kcal mol^{-1} for crotyl alcohol, 14 kcal mol^{-1} for butanol, and 12 kcal mol^{-1} for C_3 hydrocarbons

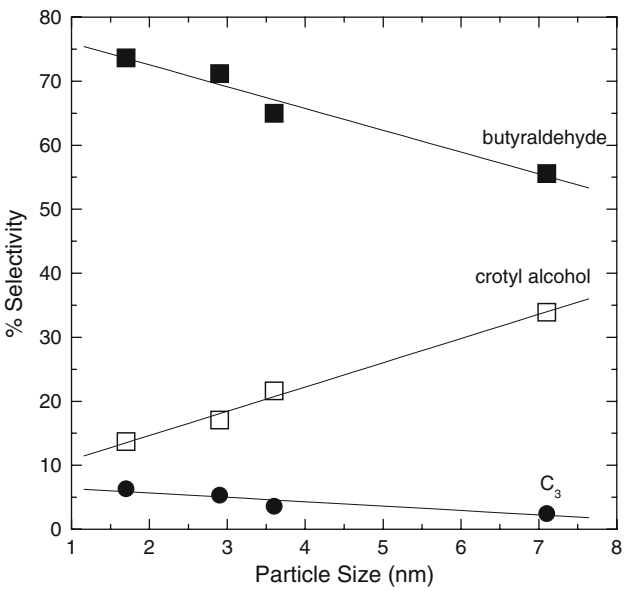

Fig. 2 Selectivity as a function of particle size at 353 K for butyraldehyde (■), crotyl alcohol (□), and C_3 hydrocarbons (●). The selectivity towards crotyl alcohol increased with increasing particle size, while the butyraldehyde selectivity decreased. The pressure of crotonaldehyde and hydrogen was 8 Torr and 160 Torr (760 Torr total pressure)

shown in Figs. 2 and 3 for Pt(1.7 nm)/SBA-15 and Pt(7.1 nm)/SBA-15. The overall rate and selectivity to crotyl alcohol increased monotonically with increasing particle size. The steady-state rate increased by a factor of ~2 (from 2.1 × 10 to 4.8 × 10^{-2} s^{-1}) and the selectivity towards crotyl alcohol varied by a factor of ~3 (from 13.7% to 33.9%) with an increase in the particle size from 1.7 to 7.1 nm. The increase in selectivity toward crotyl alcohol with particle size has been well-documented [10]. The preferential bonding of C=O through a di-σ interaction on the extended, close packed (111) surface and the C=C through a π-bond on the more corrugated Pt(110) surface has been determined both theoretically [14] and experimentally [26]. Larger particles have a larger proportion of extended (111) terraces, while smaller particles have a larger fraction of edge and corner sites.

The initial deactivation is also dependent on particle size. During the first few minutes on stream, Pt(1.7 nm)/SBA-15 is 1.5 times more active than Pt(7.1 nm)/SBA-15 (6.9 × 10^{-2} s^{-1} vs. 4.7 × 10^{-2} s^{-1} at 353 K). While both catalysts have the same TOF for butyraldehyde production, the Pt(1.7 nm)/SBA-15 is 1.5 times more active for the formation of crotyl alcohol, seven times more active for complete hydrogenation to butanol, and three times more active for decarbonylation at the onset of the reaction (Fig. 4). The three-fold higher specific activity for decarbonylation explains the larger extent of deactivation over Pt(1.7 nm)/SBA-15 compared to Pt(7.1 nm)/SBA-15. The

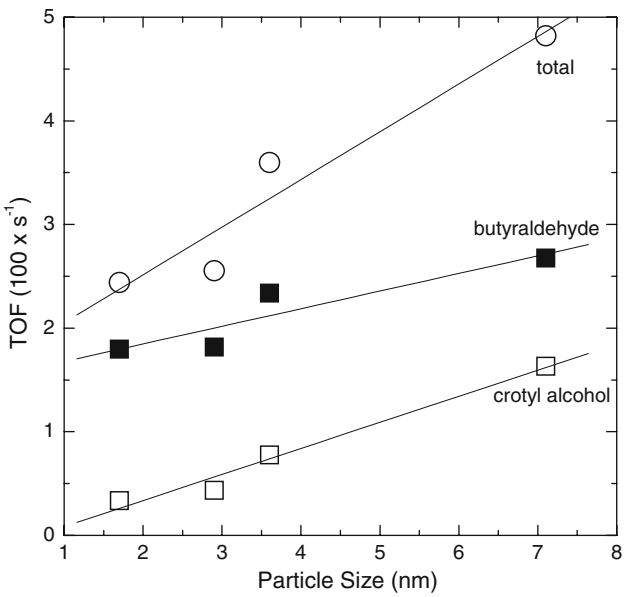

Fig. 3 Turnover frequency as a function of particle size at 353 K for butyraldehyde (■) and crotyl alcohol (□). The overall TOF (○) increases with particle size, but more strongly for the formation of crotyl alcohol. The pressure of crotonaldehyde and hydrogen was 8 Torr and 160 Torr (760 Torr total pressure)

initial TOF for decarbonylation over the four catalysts is 2.5 × 10^{-3}, 1.8 × 10^{-3}, 1.0 × 10^{-3}, and 1.0 × 10^{-3} s^{-1} for Pt(1.7 nm)/SBA-15 (3.3-fold decrease in activity from initial to steady-state), Pt(2.9 nm)/SBA-15 (2.3-fold decrease), Pt(3.6 nm)/SBA-15 (1.8-fold decrease), and

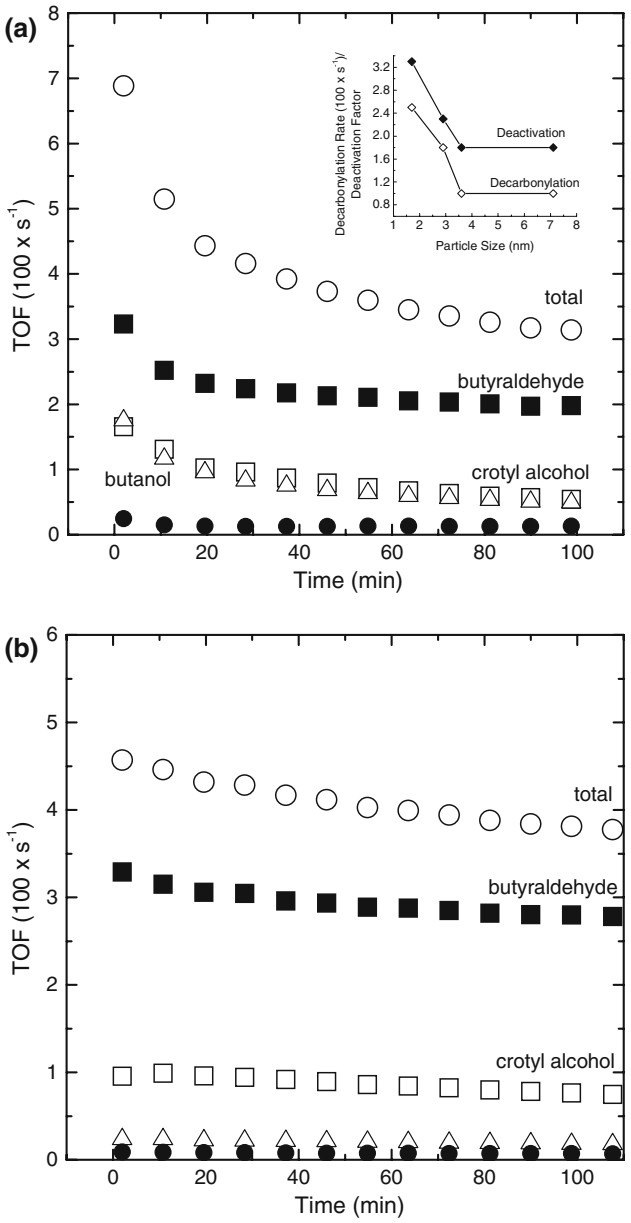

Fig. 4 Initial deactivation of (**a**) Pt(1.7 nm)/SBA-15 and (**b**) Pt(7.1 nm)/SBA-15 with time-on-stream at 353 K. The initial overall turnover frequency is greater for the 1.7 nm particles, but they demonstrate a greater extent of deactivation (presumably due to the greater rate of decarbonylation). The disappearance of crotonaldehyde (○) and the formation of butyraldehyde (■), crotyl alcohol (□), butanol (Δ), and C_3 hydrocarbons (●) are shown. The inset shows the initial rate of decarbonylation () and the amount of deactivation, expressed as initial rate/steady-state rate (disappearance of crotonaldehyde) for each of the four Pt(*X*)/SBA-15 catalysts. The pressure of crotonaldehyde and hydrogen was 8 Torr and 160 Torr (760 Torr total pressure)

Pt(7.1 nm)/SBA-15 (1.8-fold decrease), respectively (inset in Fig. 4a). After this initial deactivation period, the decarbonylation rate over all four catalysts is the same. This suggests that over longer time scales, the decreased activity of Pt(1.7)/SBA-15 results from coke formation. The increased amount of decarbonylation and coke formation over the smaller 1.7 nm particles likely results from the increased C–C bond scission activity of low-coordination sites that predominate on smaller nanoparticles.

3.4 CO Poisoning

CO poisoning was tested over the series of catalysts by the addition of small quantities of CO to the feed. Reaction rates were measured over Pt(1.7 nm)/SBA-15 and Pt(7.1 nm)/SBA-15 at 353 K as described above with the addition of a low pressure of CO (134–262 mTorr CO). For both catalysts, the overall reaction rate dropped by ~70% in the presence of 134 mTorr CO relative to the rate before addition of CO. The rate of formation of C_3 hydrocarbons and butanol in the presence of CO was detectable, but too low for accurate rate determination. The reaction order at 353 K in CO on the Pt(1.7 nm)/SBA-15 was −0.9 and −1.4 for butyraldehyde and crotyl alcohol, respectively, For the Pt(7.1)/SBA-15, the reaction order in CO was −0.9 for both products (Fig. 5). The reaction order of ≤−1 suggests that CO is the most abundant surface intermediate during crotonaldehyde hydrogenation in the presence of 130–260 mTorr CO [27]. Although the partial pressure of CO reached during reaction conditions in the absence of CO via decarbonylation (~15 mTorr) is much lower than the pressures used here, it is reasonable to assume that CO acts as a poison in that case as well. The more negative reaction order for crotyl alcohol formation over Pt(1.7)/SBA-15 is not currently understood, but does coincide with the observation that the initial rate of formation of crotyl alcohol over Pt(1.7)/SBA-15 is very high (three times higher than observed over Pt(7.1)/SBA-15), but decreases to a rate three times lower than that observed over Pt(7.1)/SBA-15.

3.5 Effect of Reduction Temperature on Catalyst Activity and Selectivity

The effect of reduction temperature was studied on both Pt(*X* nm)/SBA-15 catalysts. All samples were calcined in O_2 at high temperature followed by reduction in H_2 (as described previously) in the reactor immediately prior to reactivity studies of crotonaldehyde hydrogenation. All samples show an optimal reduction temperature of ~673–723 K with lower and higher reduction temperatures resulting in a lower overall conversion rate of crotonaldehyde as well as a lower selectivity towards crotyl alcohol (Fig. 6). Particle sintering, which has been observed in many studies of Pt on SiO_2 [28], is ruled out as the cause of these changes based on TEM observations of the catalysts before and after high temperature reduction.

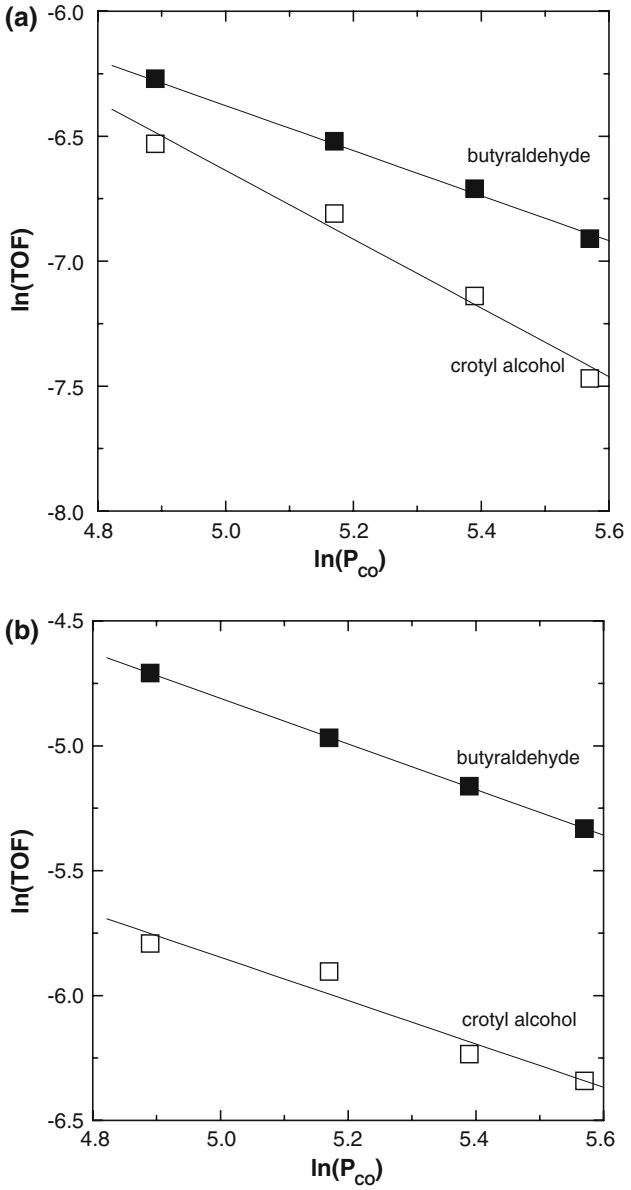

Fig. 5 The dependence of the rate of butyraldehyde (■) and crotyl alcohol (□) formation on the pressure of CO for (**a**) Pt(1.7 nm)/SBA-15 and (**b**) Pt(7.1 nm)/SBA-15. The reaction conditions were 353 K, 8 Torr crotonaldehyde, 160 Torr H_2, 134–262 mTorr CO in a balance He

The fact that a strong dependence on particle size is observed for this series of Pt(*X*)/SBA-15 catalysts suggests that PVP is acting in a fashion similar to the oxidized carbon support studied by Coloma et al. [29] Some oxidized carbon likely remains on the Pt nanoparticle surface even after high temperature calcination. In a study of PVP capped Pt nanoparticles, after heating in N_2 at 773 K for 0.5 h, 38.2% of the original C and 39.9% of the original O from PVP remained in the sample [21]. In fact, in that study, which employs a similar nanoparticle synthesis, the Pt content of the sample was initially only 10.5% by weight

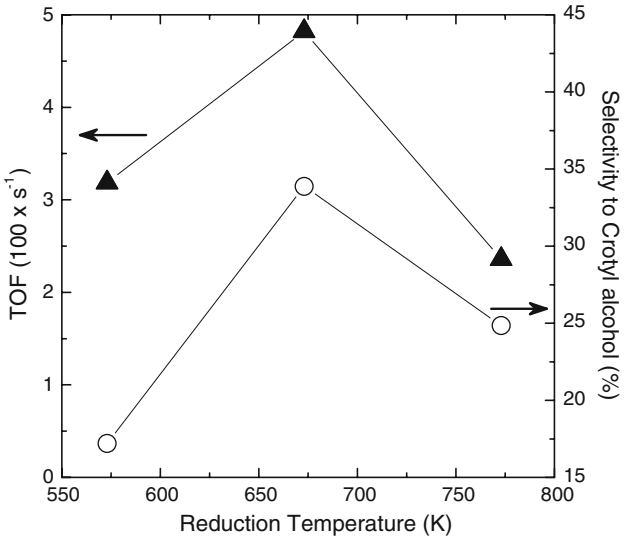

Fig. 6 Overall turnover frequency (▲) and selectivity (○) to crotyl alcohol as a function of reduction temperature Pt(7.1 nm)/SBA-15. The overall TOF is maximized when the catalysts are reduced at temperatures of 573–773 K. The pressure of crotonaldehyde and hydrogen was 8 Torr and 160 Torr (760 Torr total pressure) and 353 K

and increased to only 25.8% after the high temperature treatment in N_2. This suggests that a significant amount of oxidized carbon is likely in contact with the Pt nanoparticles during the reaction studies we have carried out.

The residual oxidized carbon left behind by the partial decomposition of PVP likely undergoes varying degrees of reduction depending on the temperature of the H_2 pretreatment. Borodko et al. [30] have shown that the carbonyl group of PVP interacts mores strongly with Pt nanoparticles when oxidized in air at 363 K than when reduced in H_2 at 363 K and this process is reversible. As the reduction temperature increases, the oxygenated groups of this residual layer may become hydrogenated while upon further temperature increase, the carbon overlayer may densify with complete loss of oxygenated groups, thus deactivating the catalyst by a mechanism similar to coking. The role of stabilizing molecules is important and has not been adequately studied for use of colloidally prepared NPs in gas-phase heterogeneous catalysis. Even after thermal treatment in O_2 at 623–723 K, some organic overlayer remains on the Pt surface and is modified by subsequent H_2 treatment.

4 Conclusions

Monodisperse Pt nanoparticles (1.7–7.1 nm) synthesized by the alcohol reduction method in the presence of poly(vinylpyrrolidone) were supported on mesoporous SBA-15 silica for of the hydrogenation of crotonaldehyde.

The solution phase synthesis of Pt nanoparticles provided excellent control over particle size and particle size distribution, allowing for better understanding of the effect of particle size on selectivity in catalysis. Both the activity and selectivity towards crotyl alcohol increased with increasing particle size. As the particle size increased from 1.7 to 7.1 nm, the turnover frequency increased from 2.1×10^{-2} to 4.8×10^{-2} s^{-1} and the selectivity to crotyl alcohol increases from 14% to 34% (353 K and H_2/crotonaldehyde ratio of 20). The initial rate of decarbonylation is also particle size dependent: the TOF is 2.5×10^{-3} over Pt(1.7 nm)/SBA-15 and only 1.0×10^{-3} over Pt(7.1 nm)/SBA-15. The enhanced rate of decarbonylation over catalysts with smaller Pt particles appears to be responsible for the increased deactivation; this is corroborated by CO poisoning experiments which show that the reaction order in CO -1 to -1.4 for the formation of butyraldehyde and crotonaldehyde. The reduction temperature significantly influenced both the activity and selectivity; there is an optimal reduction temperature of $\sim$673–723 K for both 1.7 and 7.1 nm Pt nanoparticle catalysts.

Acknowledgments This work was supported by the Director, Office of Science, Office of Basic Energy Sciences, Division of Chemical Sciences, Geological and Biosciences of the U.S. Department of Energy under Contract No. DE-AC03-76SF00098. This work was also supported by the Director, Office of Science, Office of Basic Energy Sciences, Division of Materials Sciences and Engineering of the U.S. Department of Energy under Contract No. DE-AC02-05CH11231.

References

1. Aiken JD, Finke RG (1999) J Mol Catal A: Chem 145:1
2. Roucoux A, Schulz J, Patin H (2002) Chem Rev 102:3757
3. Lang HF, May RA, Iversen BL, Chandler BD (2003) J Am Chem Soc 125:14832
4. Konya Z, Puntes VF, Kiricsi I, Zhu J, Ager JW, Ko MK, Frei H, Alivisatos P, Somorjai GA (2003) Chem Mater 15:1242
5. Rioux RM, Song H, Hoefelmeyer JD, Yang P, Somorjai GA (2005) J Phys Chem B 109:2192
6. Song H, Rioux RM, Hoefelmeyer JD, Komor R, Niesz K, Grass M, Yang PD, Somorjai GA (2006) J Am Chem Soc 128:3027
7. Rioux RM, Hoefelmeyer JD, Grass M, Song H, Niesz K, Yang PD, Somorjai GA (2008) Langmuir 24:198
8. Rioux RM, Komor R, Song H, Hoefelmeyer JD, Grass M, Niesz K, Yang PD, Somorjai GA (2008) J Catal 254:1
9. Grass ME, Yue Y, Habas SE, Rioux RM, Teall CI, Yang P, Somorjai GA (2008) J Phys Chem C 112:4797
10. Gallezot P, Richard D (1998) Cat Rev Sci Eng 40:81
11. Santori GF, Casella ML, Siri GJ, Aduriz HR, Ferretti OA (2002) React Kinet Catal Lett 75:225
12. Giroir-Fendler A, Richard D, Gallezot P (1990) Catal Lett 5:175
13. Englisch M, Jentys A, Lercher JA (1997) J Catal 166:25
14. Delbecq F, Sautet P (1995) J Catal 152:217
15. Venezia AM, Liotta LF, Pantaleo G, La Parola V, Deganello G, Beck A, Koppany Z, Frey K, Horvath D, Guczi L (2003) Appl Catal A: Gen 251:359
16. Deutsch DS, Siani A, Fanson PT, Hirata H, Matsumoto S, Williams CT, Amiridis MD (2007) J Phys Chem C 111:4246
17. Song H, Kim F, Connor S, Somorjai GA, Yang PD (2005) J Phys Chem B 109:188
18. Wang Y, Ren J, Deng K, Gui L, Tang Y (2000) Chem Mater 12:1622
19. Teranishi T, Hosoe M, Tanaka T, Miyake M (1999) J Phys Chem B 103:3818
20. Grubbs RB (2007) Polym Rev 47:197
21. Du YK, Yang P, Mou ZG, Hua NP, Jiang L (2006) J Appl Poly Sci 99:23
22. Birchem T, Pradier CM, Berthier Y, Cordier G (1994) J Catal 146:503
23. Waghray A, Blackmond DG (1993) J Phys Chem 97:6002
24. Singh UK, Vannice MA (2000) J Catal 191:165
25. Shekhar R, Barteau MA (1994) Surf Sci 319:298
26. Beccat P, Bertolini JC, Gauthier Y, Massardier J, Ruiz P (1990) J Catal 126:451
27. Boudart M (1972) AIChE J 18:465
28. Baker RTK, Prestridge EB, Garten RL (1979) J Catal 56:390
29. Coloma F, Sepulveda-Escribano A, Fierro JLG, Rodriguez-Reinoso F (1997) Appl Catal A: Gen 150:165
30. Borodko Y, Humphrey SM, Tilley TD, Frei H, Somorjai GA (2007) J Phys Chem C 111:6288